J|A|C|S
ARTICLES
Published on Web 07/19/2002

X-ray Reflectivity and Diffraction Studies on Lipid and Lipopolymer Langmuir−Blodgett Films under Controlled Humidity

Jörg Bolze,*,†,‡ Masamitu Takahasi,§ Jun'ichiro Mizuki,§ Tobias Baumgart,|| and Wolfgang Knoll||

Contribution from the RIKEN Harima Institute/SPring-8, Structural Biophysics Laboratory, 1-1-1 Kouto, Mikazuki-cho, Sayo-gun, Hyogo 679-5148, Japan, Pohang Accelerator Laboratory, Pohang University of Science and Technology (POSTECH), San 31, Hyoja-dong, Pohang 790-784, Korea, Japan Atomic Energy Research Institute (JAERI), 1-1-1 Kouto, Mikazuki-cho, Sayo-gun, Hyogo 679-5148, Japan, and Max-Planck-Institut für Polymerforschung, Ackermannweg 10, 55128 Mainz, Germany

Received April 15, 2002

Abstract: Synchrotron X-ray reflectivity and grazing incidence diffraction were applied to study the structures of phospholipid Langmuir−Blodgett films under controlled humidity. Distearoylphosphatidylethanolamine (DSPE) and DSPE−PEO lipopolymers, in which a poly(ethylene oxide) chain with $n = 8$, 17, or 45 EO units is covalently linked to the polar headgroup of DSPE, were used. When the relative humidity was changed from below 2 to 97%, the phosphate headgroup in a DSPE film was hydrated with a concomitant thickness increase of 4.2 Å and an electron density decrease. The swelling of the monolayer was found to be a reversible process without any significant roughening of the film. Subtle differences in the film thickness could be detected for DSPE monolayers transferred under various lateral pressures. The degree of lateral ordering of the alkyl chains in DSPE monolayers increased considerably when the humidity was raised. In the case of DSPE−PEO with eight EO units, the hydration of the monolayer was also found to be reversible, but the water uptake was larger due to the presence of the hydrophilic polymer interlayer, which is located between the substrate and the DSPE moieties. Under high humidity, the lipopolymer monolayer with $n =$ 17 exhibited a well-defined, layered structure similar to that of DSPE−PEO with $n = 8$. In the case of $n =$ 45, however, there are indications for a significant intermixing of the polymer with the DSPE moieties, probably resulting in the formation of hydrophobic nanodomains of closely packed alkyl chains that are immersed into the hydrated polymer.

Introduction

Planar, polymer-supported lipid membranes attached to a substrate are highly interesting model membrane systems for both scientific and practical applications.[1−3] They retain key features of biological membranes such as lateral fluidity and a high water activity on both sides of the membrane. A hydrophilic polymer cushion is introduced in order to decouple the membrane from the substrate[4] and to provide a soft, water-rich environment for biomolecules. The polymer may be tethered to the substrate on the bottom side and to the lipid membrane on top by either chemi- or physisorption.[1] Integral membrane proteins may be incorporated, and their activity may be studied.[1,3]

Lipopolymers, in which a poly(ethylene oxide) (PEO) chain is chemically bonded to the polar head of a phospholipid molecule, are commercially available. They form monolayers at the air−water interface, which may be transferred onto a solid substrate by the Langmuir−Blodgett (LB) technique to yield a polymer-cushioned lipid monolayer.[5] Those monolayers may be either physisorbed or chemically coupled to the underlying support.[6,7] In a subsequent step, a second lipid monolayer may be deposited on top of the LB film (e.g., by the spreading of vesicles or by the Langmuir−Schäfer technique) to yield a polymer-cushioned, bilayer membrane on a solid substrate.[7,8]

The stable, planar configuration of such systems allows their structural characterization with a combination of many modern

* To whom correspondence should be addressed. Current address: Polymer-Institut, Universität Karlsruhe, Kaiserstr. 12, 76128 Karlsruhe, Germany. (Tel) +49 721 608 3151; (fax) +49 721 608 3153; (e-mail: bolze@polyibm2.chemie.uni-karlsruhe.de.
† RIKEN Harima Institute/SPring-8.
‡ Pohang University of Science and Technology.
§ Japan Atomic Energy Research Institute.
|| Max-Planck-Institut für Polymerforschung.

(1) Knoll, W.; Frank, C. W.; Heibel, C.; Naumann, R.; Offenhäusser, A.; Rühe, J.; Schmidt, E. K.; Shen, W. W.; Sinner, A. *J. Mol. Biotechnol.* **2000**, *74*, 137−158 and references given therein.
(2) Sackmann, E. *Science* **1996**, *271*, 43−48.
(3) Sackmann, E.; Tanaka, M. *Tibtech* **2000**, *18*, 58−64.
(4) Kühner, M.; Rampe, R.; Sackmann, E. *Biophys. J.* **1994**, *67*, 217−226.
(5) Baekmark, T. R.; Elender, G.; Lasic, D. D.; Sackmann, E. *Langmuir* **1995**, *11*, 3975−3987.
(6) Naumann, C. A.; Prucker, O.; Lehmann, T.; Rühe, J.; Knoll, W.; Frank, C. W. *Biomacromolecules* **2002**, *3*, 27−35.
(7) Wagner, M. L.; Tamm, L. K. *Biophys. J.* **2000**, *79*, 140−1414.
(8) Sinner, A.; Offenhäusser, A. *Thin Solid Films* **1998**, *327−329*, 758−761.

10.1021/ja0265308 CCC: $22.00

surface-sensitive analytical tools[1,2] such as evanescent wave optics, light, X-ray, and neutron reflectometries, in-plane X-ray diffraction, vibrational spectroscopy, fluorescence microscopy, scanning probe microscopies, or impedance spectroscopy.

The preparation procedure for polymer-supported lipid membranes inevitably includes a drying step after the LB transfer. It is therefore important to investigate the nature, magnitude, and reversibility of dehydration and rehydration in lipid and lipopolymer monolayers. The hydration of amphiphile monolayers on a substrate was examined by Chen and Israelachvili in humid air by using the surface force apparatus.[9] It was found that water, which penetrates into the monolayer, can lift the monolayer off the surface, leading to an increased film thickness and to a reduced adhesion between monolayer and substrate. The influence of relative humidity on the properties of polymer-supported amphiphile monolayers on a substrate was investigated by Chi et al.[10] They could show that a hydrated polyethyleneimine interlayer increases the mobility within the membrane. There are also detailed reports on ellipsometric thickness measurements of polymer-supported lipid monolayers as a function of the humidity.[5,11] Kinetic measurements by Hausch et al.[12] allowed monitoring of the incorporation of water into lipopolymer monolayers by means of surface plasmon spectroscopy.

X-ray and neutron reflectivities (XR, NR)[13−15] have proven to be very powerful tools to study the structure of ultrathin films. Using these methods, the film thickness may be determined independently from the refractive index. This is a great advantage over optical methods, such as ellipsometry or surface plasmon spectroscopy,[16] where the film thickness and the refractive index are strongly correlated, so that only an optical thickness may be obtained. Furthermore, XR and NR allow determination of scattering length density profiles along the film surface normal with a high resolution. Information about the lateral order within monolayers can be obtained by grazing incidence X-ray diffraction (GIXD).[17] Combined reflection and diffraction measurements have been conducted extensively to study the structures of various lipid monolayers floating at the air−water interface in a Langmuir trough. It has become possible to reveal structural transitions all along the pressure−area isotherm from the laterally isotropic fluid to the ordered phases.[17−24] Recently, floating lipopolymer and mixed lipid/lipopolymer monolayers were investigated with the same methods, under variation of the lateral pressure, the polymer chain length, and the mixing ratio.[25−30] On the other hand, the number of reported reflectivity and diffraction studies on lipid mono- or bilayers transferred on a solid substrate, is still rather limited. A few interesting works on such systems have appeared quite recently, however.[22,30−36]

Thanks to the availability of high-brilliance synchrotron X-ray radiation sources, reflectivities may now be measured down to $R \sim 10^{-10}$, which allows one to probe larger angles with a concomitantly higher spatial resolution approaching the atomic level.[30] This is particularly important for studies of ultrathin films with a thickness of a few nanometers only, where the characteristic oscillations in a reflectivity curve have rather large spacings. The high beam intensity also greatly facilitates measuring the weak diffraction signals from a monolayer. However, it has to be kept in mind that organic material is prone to be damaged by X-ray radiation.[37] Special care is required to investigate any effects of radiation damage before data interpretation is done.

In this work, we report about the characterization of DSPE and DSPE−PEO Langmuir−Blodgett films by X-ray reflectivity and grazing incidence X-ray diffraction using synchrotron radiation. Those measurements were done under controlled humidity in order to study the extent, location, and reversibility of water incorporation in the monolayers. Lipopolymers with three different polymer chain lengths (number of EO units $n =$ 8, 17, and 45) were investigated.

Experimental Section

The phospholipid distearoylphosphatidylethanolamine (DSPE) and the lipopolymers DSPE−PEO,[27] which contain a poly(ethylene oxide) chain chemically grafted to the terminal amine of the headgroup of DSPE, were used. The number-average molecular weights of the PEO chains were 350, 750, and 2000, corresponding to $n = 8$, 17, and 45 monomer units, respectively. In the following, those lipopolymers will be shortly denoted as DSPE−PEO(350), DSPE−PEO(750), and DSPE−PEO(2000). Silicon (100) wafers were thermally oxidized to yield an oxide layer thickness of ∼50 or 150 nm. For the preparation of Langmuir−Blodgett monolayers, a Langmuir trough thermostated at 25 °C was used. The lipids were dissolved in a mixture of chloroform and methanol and then spread on the water subphase. The measured

(9) Chen, Y.-L.; Israelachvili, J. *J. Phys. Chem.* **1992**, *96*, 7752−7760.
(10) Chi, L. F.; Johnston, R. R.; Ringsdorf, H. *Langmuir* **1992**, *8*, 1360−1365.
(11) Mathe, G.; Gege, C.; Neumaier, K. R.; Schmidt, R. R.; Sackmann, E. *Langmuir* **2000**, *16*, 3835−3845.
(12) Hausch, M.; Zentel, R.; Knoll, W. *Macromol. Chem. Phys.* **1999**, *200*, 174−179.
(13) Daillant, J., Gibaud, A., Eds. *X-ray and neutron reflectivity: principles and applications*; Springer-Verlag: Berlin, 1999; and references given therein.
(14) Holy, V.; Pietsch, U.; Baumbach, T. *High-resolution X-ray scattering from thin films and multilayers*; Springer-Verlag: Berlin, 1999; and references given therein.
(15) Tolan, M. *X-ray scattering from soft matter thin films;* Springer-Verlag: Berlin, 1999; and references given therein.
(16) Rothenhäusler, B.; Knoll, W. *J. Appl. Phys.* **1988**, *67*, 3572−3575.
(17) Helm, C. A.; Tippmann-Krayer, P.; Möhwald, H.; Als-Nielsen, J.; Kjaer, K. *Biophys. J.* **1991**, *60*, 1457−1476.
(18) Brezesinski, G.; Bringezu, F.; Weidemann, G.; Howes, P. B.; Kjaer, K.; Möhwald, H. *Thin Solid Films* **1998**, *327−329*, 256−261.
(19) Helm, C. A.; Möhwald, H.; Kjaer, K.; Als-Nielsen, J. *Europhys. Lett.* **1987**, *4*, 697−703.
(20) Helm, C. A.; Möhwald, H.; Kjaer, K.; Als-Nielsen, J. *Biophys. J.* **1987**, *52*, 381−389.
(21) Krueger, S. *Curr. Opin. Colloid Interface Sci.* **2001**, *6*, 111−117.
(22) Krueger, S.; Meuse, C. W.; Majkrzak, C. F.; Dura, J. A.; Berk, N. F.; Tarek, M.; Plant, A. L. *Langmuir* **2001**, *17*, 511−521.
(23) Schalke, M.; Krüger, P.; Weygand, M.; Lösche, M. *Biochim. Biophys. Acta* **2000**, *1464*, 113−126.
(24) Schalke, M.; Lösche, M. *Adv. Colloid Interface Sci.* **2000**, *88*, 243−274.
(25) Ahrens, H.; Baekmark, T. R.; Merkel, R.; Schmitt, J.; Graf, K.; Raiteri, R.; Helm, C. A. *ChemPhysChem* **2000**, *2*, 101−106.
(26) Ahrens, H.; Graf, K.; Helm, C. A. *Langmuir* **2001**, *17*, 3113−3115.
(27) Kuhl, T. L.; Majewski, J.; Howes, P. B.; Kjaer, K.; von Nahmen, A.; Lee, K. Y. C.; Ocko, B.; Israelachvilli, J. N.; Smith, G. S. *J. Am. Chem. Soc.* **1999**, *121*, 7682−7688.
(28) Majewski, J.; Kuhl, T. L.; Gerstenberg, M. C.; Israelachvili, J. N.; Smith, G. S. *J. Phys. Chem. B* **1997**, *101*, 3122−3129.
(29) Majewski, J.; Kuhl, T. L.; Kjaer, K.; Gerstenberg, M. C.; Als-Nielsen, J.; Israelachvili, J. N.; Smith, G. S. *J. Am. Chem. Soc.* **1998**, *120*, 1469−1473.
(30) Majewski, J.; Kuhl, T. L.; Wong, J. Y.; Smith, G. S. *Rev. Mol. Biotechnol.* **2000**, *74*, 207−231.
(31) Fragneto, G.; Bellet-Amalric, E.; Charitat, T.; Dubos, P.; Graner, F.; Perino-Galice, L. *Physica B* **2000**, *276−278*, 501−502.
(32) Franz, H.; Dante, S.; Wappmannsberger, Th.; Petry, W.; de Rosa, M.; Rustichelli, F. *Thin Solid Films* **1998**, *327−329*, 52−55.
(33) Haas, H.; Torrielli, M.; Steitz, R.; Cavatorta, P.; Sorbi, R.; Fasano, A.; Riccio, P.; Gliozzi, A. *Thin Solid Films* **1998**, *327−329*, 627−631.
(34) Kuhl, T. L.; Majewski, J.; Wong, J. Y.; Steinberg, S.; Leckband, D. E.; Israelachvili, J. N.; Smith, G. S. *Biophys. J.* **1998**, *75*, 2352−2362.
(35) Majewski, J.; Wong, J. Y.; Park, C. K.; Seitz, M.; Israelachvili, J. N.; Smith, G. S. *Biophys. J.* **1998**, *75*, 2363−2367.
(36) Poloucek, P.; Pietsch, U.; Geue, T.; Symietz, Ch.; Brezesinski, G. *J. Phys D: Appl. Phys.* **2001,** *34*, 450−458.
(37) Cherezov, V.; Cheng, A.; Petit, J.-M.; Diat, O.; Caffrey, M. *Cell. Mol. Biol. (Paris)* **2000**, *46*, 1133−1145.

pressure−area isotherms for DSPE and for the three different lipopolymers showed the same features as already reported by others.[25,27] The films were kept at the final pressure for at least 1 h and then transferred onto the substrates.

X-ray reflectivity and diffraction data were collected using dedicated beamlines at the synchrotron radiation facilities SPring-8 (BL14,[38] Japan) and at the Pohang Light Source (BL3C2,[39] Korea). A specially designed sample cell was mounted in the center of the diffractometer on a small goniometer head. The X-rays can penetrate and exit the cell through windows made of a thin polyimide film. To adjust the relative humidity to 97%, a glass vessel containing a saturated K_2SO_4 solution was placed at the bottom of the tightly sealed sample cell. A relative humidity below 2% was achieved using $CaSO_4$ as a desiccant. A precise sample alignment was done as described elsewhere.[40]

X-ray reflectivity was measured by scanning the tilt angle α of the (horizontal) sample surface with respect to the primary beam direction and by simultaneously moving the detector arm by 2α. Thus, the scattering vector $\bar{q}$ only has a component vertically to the sample surface (z-direction; $q_z = 4\pi/\lambda \cdot \sin\alpha$, where λ is the wavelength of radiation) and the electron density profile along the film surface normal is probed. Reflectivities R, i.e., the ratio of the reflected and incident beam intensities, were calculated in the kinematic approximation.[42] Box models were used to parametrize the electron density distribution in the monolayer along the surface normal.[17] Each box with a certain length represents a region of quasi-constant density. Interface roughness was modeled using error functions, and the mean square interface width (σ^2) is given by the second moment of the electron density gradient. Parameters in the least-squares fitting procedure of the experimental data were the electron density and thickness of each box, as well as the roughness parameters between adjacent boxes.

Grazing incidence X-ray diffraction[41] probes for lateral, quasi-periodic order in the film. The incident angle is fixed at a value slightly smaller than the critical angle[15] of silicon. Bragg peaks are measured by scanning the detector in the xy-plane and simultaneously integrating over the signal along the vertical direction. The repeat distances d of the lattice structure are related to the peak position by $d = 2\pi/q_{xy}$, and the lateral correlation length ξ is inversely proportional to the peak width. The magnitude of the horizontal scattering vector is given by $q_{xy} = 4\pi/\lambda \cdot \sin\theta_{xy}$, where $2\theta_{xy}$ represents the in-plane scattering angle between the incident and diffracted beam.

Results and Discussion

Radiation Damage and Data Reproducibility. X-ray radiation from synchrotron sources was used for the purpose of studying minute structural changes in ultrathin organic films as a function of sample preparation and sample environment conditions. Due to the high brightness of the X-ray beam, XR data become available in an extended angular region with a concomitantly increased spatial resolution approaching the atomic level. On the other hand, the interaction between ionizing radiation and organic materials may lead to considerable radiation damage,[23,37] which is believed to proceed through the generation and chain reactions of free radicals.[43] It is thus mandatory to carefully check for possible effects of radiation damage as well as for the reproducibility of experimental data.

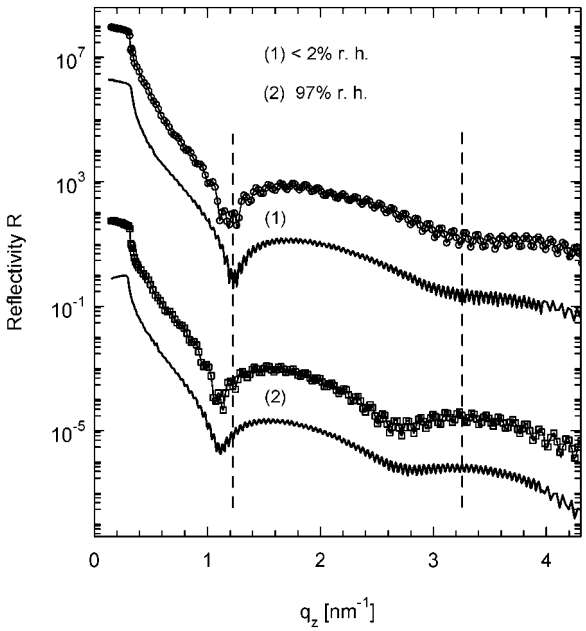

Figure 1. Demonstration of the good reproducibility of XR data measured at different relative humidities (r.h.) and also at different experimental stations, respectively. Shown here as an example are the measured data from LB films of DSPE (π = 42 mN/m). Sample preparation and measurement procedures were the same, the only difference being the thermal SiO_x layer thickness. Connected marks: measurements at PLS, $d(SiO_x) \sim 50$ nm; Lines: measurements at SPring-8, $d(SiO_x) \sim 150$ nm. For the sake of clarity, the curves were vertically offset.

By measuring XR profiles from various areas of the sample surface, we carefully verified that all LB films were laterally highly homogeneous (at least on the length scale of 1 mm) over the entire sample area. This enabled us to minimize the exposure on a certain area by laterally translating the sample during the course of a measurement: After sample alignment was completed, data collection was started with irradiation on a neighboring film area. For each sample, the data reproducibility was checked by repeated scans in a characteristic angular region, typically where a minimum in the XR curve occurred. In case of poor reproducibility, the original data were discarded and the curve was measured again after a horizontal translation of the sample and confirming that the sample alignment was still good. It was found that lipopolymer monolayers were more prone to radiation damage the longer the polymer chain. Measurements under dry conditions and in a high-humidity environment were conducted using the identical samples, but different areas were illuminated. We have also checked the data reproducibility by comparing the XR curves measured from the same monolayers at the two different beamlines (BL14, BL3C2). For this purpose, two different samples were used, but the preparation procedures were identical. Figure 1 compares such data measured from a DSPE monolayer under dry condition as well as under 97% relative humidity. As can be seen, the experimental data were well reproducible including even minute changes in the angular positions of the minimums as a function of the humidity. This shows the good reliability of sample preparation, humidity adjustment, and data collection procedures.

Lipid Monolayers (DSPE). X-ray Reflectivity. LB films of DSPE were prepared under lateral pressures π of 12 and 42 mN/m during monolayer transfer. Figure 2a shows the XR data measured from the sample that was transferred at 12 mN/m.

(38) Nishihata, Y.; Konishi, H.; Mizuki, J. *JAERI−Rev.* **2001**, *2001−2003*, 86.
(39) Park, B.-J.; Rah, S.-Y.; Park, Y.-J.; Lee, K.-B. *Rev. Sci. Instrum.* **1995**, *66*, 1722−1724.
(40) Bolze, J.; Ree, M.; Youn, H. S.; Chu, S.-H.; Char, K. *Langmuir* **2001**, *17*, 6683−6691.
(41) Feidenhans'l, R. *Surf. Sci. Rep.* **1989**, *10*, 105−188.
(42) Als-Nielsen, J.; Kjaer, K. In *The Proceedings of the NATO Advanced Study Institute, Phase Transitions in Soft Condensed Matter*; Geilo, Norway, April 4−14, 1989; Plenum Publishing Corp.: New York, 1989; pp 113−137.
(43) Cheng, A.; Caffrey, M. *Biophys. J.* **1996**, *70*, 2212−2222.

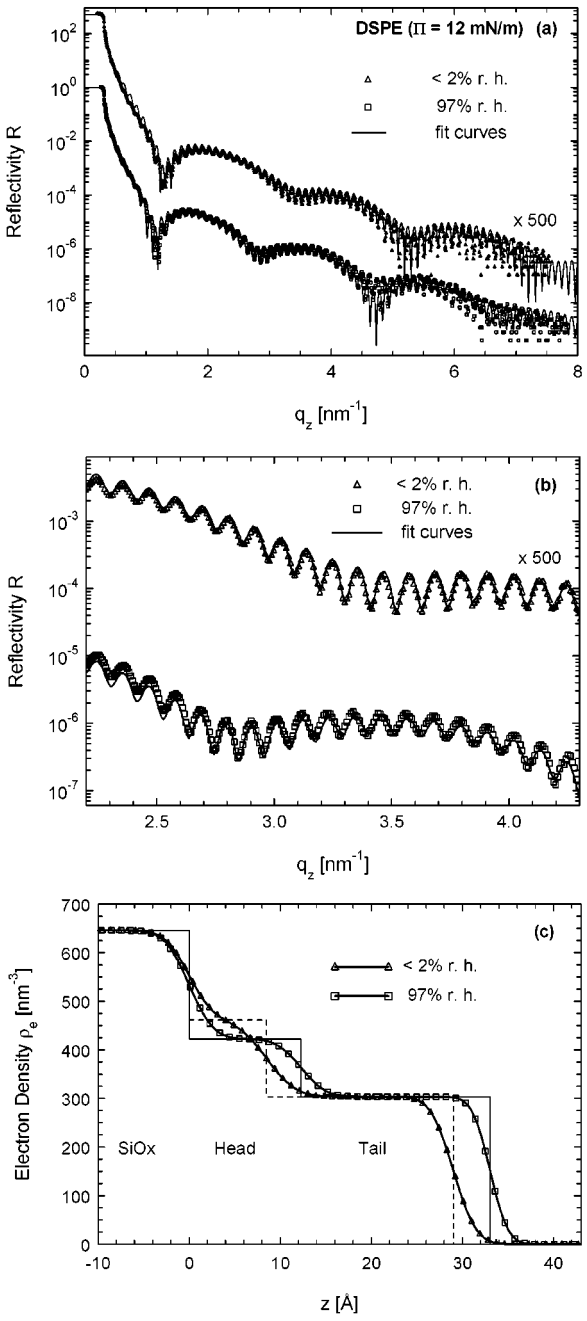

Figure 2. (a) XR data from an LB film of DSPE (π = 12 mN/m) under controlled humidity. The increase of the film thickness upon increasing the humidity is evidenced by the shift of the minimums to smaller angles. The phosphate headgroup is hydrated, and its thickness increases by 3.8 Å. Concomitantly, the electron density in the region of the phosphate group decreases. (b) A closeup of those data, displayed in a smaller angular range. (c) Fitted electron density profiles.

Displayed are the curves that were obtained under dry conditions and at 97% relative humidity, respectively. The decay of the curves with increasing angle is modulated by a high-frequency oscillation and in addition by at least one low-frequency oscillation. These oscillations, commonly known as Kiessig fringes,[44] result from the interference of X-ray beams that are reflected at different depths of the film where electron density gradients occur. The oscillation frequencies are proportional to the various distances of the interfaces, from where the reflections occur. Evidently, the high-frequency oscillations appear due to the presence of the relatively thick silicon oxide layer (~50 nm).

The XR curves were fitted with a box model for the electron density profile, which includes the silicon substrate and in addition three boxes to describe the silicon oxide layer, the phosphate headgroups, and the aliphatic tails of the lipid molecules, respectively. The polar headgroup layer is adjacent to the silicon oxide layer, whereas the box for the aliphatic tails is facing the air. In the case of the dry monolayer, the thickness of the lipid headgroup layer was determined to 8.5 Å, which is in reasonable agreement with the estimated diameter of this molecular group.[19] The thickness of the box, which is attributed to the aliphatic lipid tails, was fitted to 20.5 Å. This value should be compared with the thickness calculated under the assumption that the C_{17} alkyl chains are densely packed, in their all-trans configuration, and vertically oriented. The thickness of the hydrocarbon layer is then expected to be[45]

$$d(\text{tail}) = (16 + 9/8) \times 1.265\ \text{Å} = 21.7\ \text{Å}$$

The fact that the fitted value is by 1.2 Å smaller than the calculated one could indicate that the alkyl chains are not entirely in their all-trans conformations. This would be plausible because the molecular area at the transfer pressure of 12 mN/m is still slightly larger than that of closely packed alkyl chains. In addition, a small tilt of the molecules away from the surface normal could be assumed.

Upon increasing the relative humidity to 97%, small shifts of the minimum positions in the XR curve toward smaller angles could be observed. This indicates the increase of the monolayer thickness due to the incorporation of water. It was found that the thickness of the headgroup region increases by 3.8 Å, which equals 45% of the dry headgroup layer thickness. At the same time, the electron density in that layer decreases because the electron density of water is considerably lower than that of the headgroup. The fitted electron density in the hydrated headgroup region is in quantitative agreement with the value calculated from the fitted electron density of the dry headgroup, the known electron density of water (334 nm^{-3}), and the fitted volume increase. So the fit parameters that were obtained for the sample under dry and high-humidity conditions, respectively, are well consistent. The thickness and the electron density of the aliphatic tails are basically unaffected by the humidity change. This is reasonable, of course, as water molecules will interact mainly with the polar regions in the monolayer.

In addition to the experimental data, Figure 2a also displays the fitted curves that were obtained with the models described above. It can be seen that the data could be well fitted in the entire angular range that was accessible. Figure 2b shows a magnification of those data in a smaller region in order to demonstrate that the high-frequency oscillations due to the silicon oxide layer are also well matched by the respective fit curves. The low amplitude of those oscillations may be understood by the fact that the electron density difference between silicon and silicon oxide is small. Interfacial and surface roughness affects the overall decay of the reflectivity curves as well as the amplitudes of the oscillations, mainly at high angles where the reflected intensity is low. As we were also able to

(44) Kiessig, H. *Ann. Phys.* **1931**, *10*, 769−788.

(45) Kjaer, K.; Als-Nielsen, J.; Helm, C. A.; Tippman-Krayer, P.; Möhwald, H. *J. Phys. Chem.* **1989**, *93*, 3200−3206.

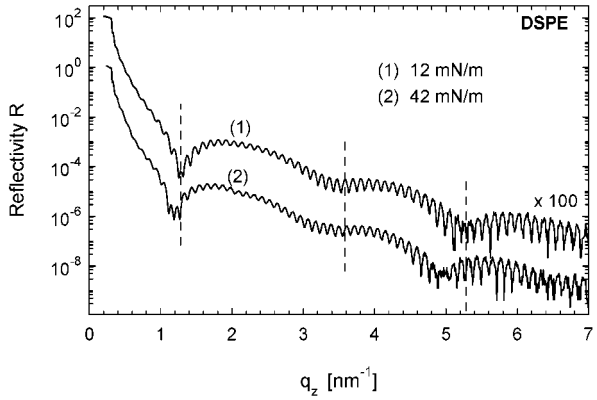

Figure 3. Comparison of the XR data measured from dry DSPE LB films that were transferred under different lateral pressures. Subtle differences observed in the angle positions of the minimums reveal a slightly higher monolayer thickness by 1.5 Å for the film transferred at the higher lateral pressure.

Table 1. Fitted Structural Parameters of the DSPE Lipid Monolayers as a Function of the Transfer Pressure π during LB Transfer and of the Adjusted Relative Humidity (r.h.)

	DSPE $\pi = 12$ mN/m <2% r.h.	DSPE $\pi = 12$ mN/m 97% r.h.	DSPE $\pi = 42$ mN/m <2% r.h.	DSPE $\pi = 42$ mN/m 97% r.h.
Electron Density ρ_e (nm^{-3})				
Si	703	703	703	703
SiO_x	646	646	646	646
Head	461	422	468	427
tail	303	303	323	323
Interface Roughness σ (Å)				
Si/SiO_x	1.5	1.5	1.5	1.5
SiO_x/head	3.0	3.0	3.0	2.5
head/tail	3.6	3.0	3.6	3.0
tail/air	2.8	2.2	3.0	3.6
Layer Thickness d (Å)				
SiO_x	535.0	532.0	547.0	514.0
head	8.5	12.3	9.0	13.0
tail	20.5	20.7	21.5	21.7
total	29.0	33.0	30.5	34.7

acquire data in this low-intensity region, detailed information about roughness could be obtained. It was found that substrate and film exhibit very smooth surfaces and interfaces, with a roughness not exceeding 3 Å under dry conditions as well as under high humidity. The fitted electron density profiles along the film surface normal are shown in Figure 2c. Here and in all other profiles displayed below, the position of the SiO_x top surface was chosen as the origin for the length scale in the vertical direction. The complete set of fit parameters is summarized in Table 1.

Figure 3 compares the XR curves measured from dry DSPE monolayers, which were transferred at 12 and at 42 mN/m, respectively. In the case of the film that was transferred at 42 mN/m, the minimums in the low-frequency oscillations appear at slightly smaller scattering vectors, which indicates that the film is slightly thicker. This may be easily understood due to the higher packing density of the molecules. Quantitatively it was found that the thickness difference is 1.5 Å, which is due to an increased thickness in both head and tail regions of the molecules.

Figure 4a displays the experimental data that were obtained from the DSPE film transferred at $\pi = 42$ mN/m at low and high humidities, respectively. Also shown are the fitted curves.

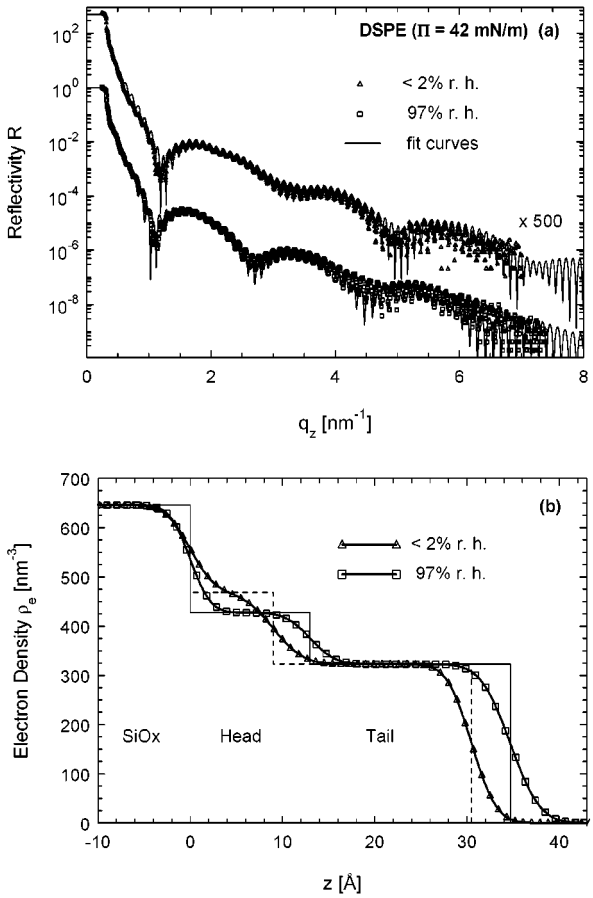

Figure 4. (a) XR data from an LB film of DSPE ($\pi = 42$ mN/m) under controlled humidity. (b) cshows the electron density profiles that correspond to the respective fit curves.

The corresponding electron density profiles are given in Figure 4b, and the complete set of fit parameters is summarized in Table 1. Beside the slightly increased thickness compared to the film that was transferred at 12 mN/m, no significant differences in the swelling capacity or in the roughness were found. The electron density that was fitted for the alkyl chains (323 nm^{-3}) is in good agreement with the corresponding value given by others[17,27] for highly compressed lipid monolayers floating at the air−water interface.

To check for the reversibility of the incorporation of water in the monolayer, the film that was initially measured under dry conditions and subsequently under 97% relative humidity was returned to the dry environment and then remeasured. Figure 5a compares the experimental data from the dry film before and after it had been exposed to high humidity for ∼20 h. Both curves coincide very well in the oscillation frequencies, the depth of the minimums, and the overall decay. This shows that the hydration of the lipid monolayer is a reversible process in which the original film thickness is restored without any significant roughening of the film.

Grazing Incidence X-ray Diffraction. The degree of lateral ordering of the alkyl chains in the DSPE monolayer transferred at 42 mN/m was probed by grazing incidence X-ray diffraction as a function of the humidity. As can be seen in Figure 6a, first-order Bragg reflections could be observed, indicating that order does exist in the monolayer. No significant change of the Bragg reflection intensities was observed upon rotating the sample around its surface normal. This indicates the existence

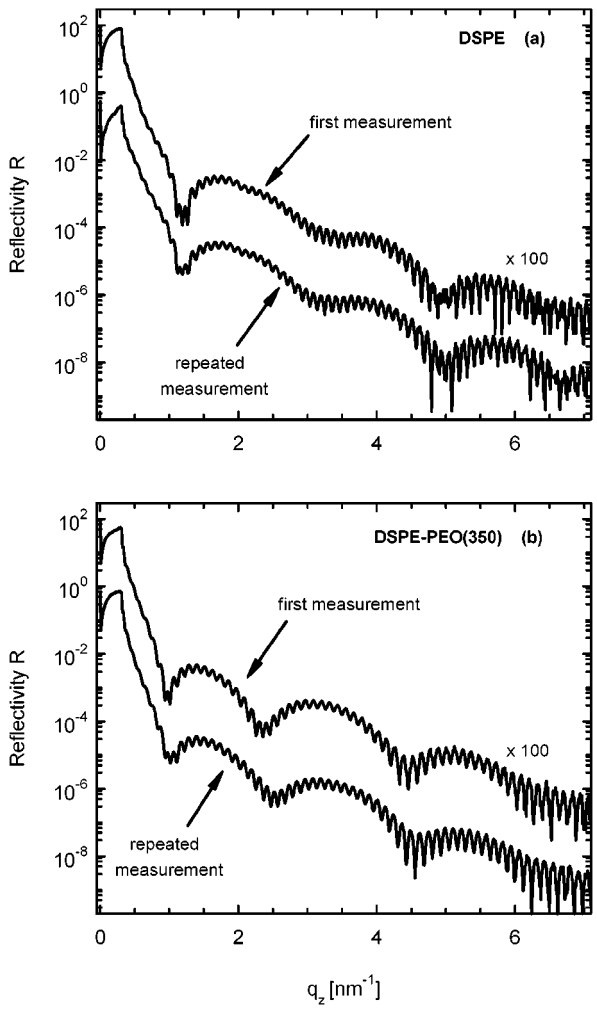

Figure 5. XR data from LB films (π = 42 mN/m) of (a) DSPE and (b) DSPE−PEO(350). The respective upper curves show the first measurements in a dry environment, whereas the lower curves were measured after the sample had been exposed for ∼20 h to 97% relative humidity and subsequently returned to the dry environment. The good reproducibility of the original data demonstrates that the hydration of the lipid and lipopolymer monolayers is a reversible process and that no significant dewetting or increase in the film roughness occurs.

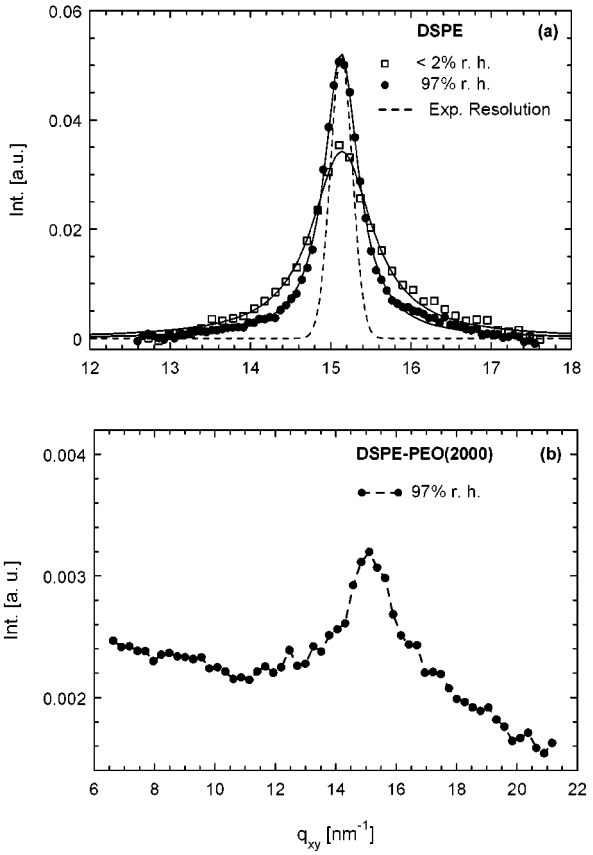

Figure 6. (a) Grazing incidence X-ray diffraction data measured from an LB film of DSPE (π = 42 mN/m) under controlled humidity. The marks indicate the experimental data, and the solid lines are Lorentzian fit curves. The dashed line represents the experimental resolution, which was obtained by a horizontal detector scan through the direct beam. A marked increase in lateral order upon increasing the humidity is observed. (b) GIXD data measured from an LB film of DSPE−PEO(2000) (π = 42 mN/m) under 97% relative humidity. Displayed are the raw data without any background subtraction. For the sake of clarity, measured data points were connected by dashed lines. The diffraction peak is very broad and indicates a positional correlation length of ∼8 Å or two molecular diameters, only. The positions of the peaks displayed in (a) and (b) only differ very slightly, indicating similar cell dimensions.

of ordered domains with a random azimuthal orientation. The Bragg spacings $d_{10} = d_{01} = d_{1-1}$ derived from the peak positions under dry conditions and at 97% relative humidity are 5.53 and 5.54 Å, respectively. These values correspond to hexagonal cell dimensions of 4.79 and 4.80 Å and to areas per diffracting unit (i.e., per alkyl chain) of 19.9 and 20.0 Å^2, respectively. These areas equal the estimated cross section of an alkyl chain (20.0 Å^2), which indicates a close packing of the alkyl chains in the monolayer. Taking into account that one lipid molecule bears two alkyl chains, the areas per lipid molecule are calculated from the above values to 39.8 and 40.0 Å^2, respectively. This is in excellent agreement with the molecular area (39 Å^2) determined from the pressure−area isotherm at the air−water interface prior to the Langmuir−Blodgett transfer of the film onto the substrate. Thus, it could be shown that the packing density is retained after film transfer. This finding was expected because the transfer ratio was very close to unity. It is also noteworthy that no significant change in the Bragg spacing occurs upon increasing the humidity. The water that is being incorporated into the monolayer leads to an increase of the film thickness, i.e., to an expansion in the vertical direction. Due to the confining effect of the substrate, however, no lateral expansion is being observed.

The line shape after deconvolution with the experimental resolution is clearly Lorentzian rather than Gaussian. This indicates a liquidlike (as opposed to crystalline) in-plane order of the alkyl chains, with an exponential decay of the positional order in real space. In this model, the lateral correlation length ζ is related to the full width at half-maximum (fwhm) of the diffraction peak by 2/fwhm.[20] The values for ζ are thus determined to 22 and 55 Å under dry conditions and 97% relative humidity, respectively. The marked increase in lateral order upon increasing the humidity is a finding that was well reproducible. It could be associated with the higher mobility of the alkyl chains in a wet environment, which promotes the energetic optimization of lateral arrangements. Due to the rather low degree of ordering, no higher order Bragg peaks could be observed. An ordered superstructure of the headgroup would give rise to half-order superlattice reflections. We searched for this reflection with a negative result.

Using GIXD, Kuhl et al.[27] determined the degree of lateral correlation in a DSPE mono-layer that is floating at the air−water interface. At an applied lateral pressure of 42 mN/m, they reported an ordered domain size of 360 Å, which is considerably larger than the value determined by us from the same monolayer after transfer on a substrate. It is important to point out, however, that Kuhl et al. used the Scherrer formula for the derivation of the correlation length from the peak width, thus assuming a crystalline order in the monolayer. This is in contrast to several other works[17,20,46] which report a Lorentzian line shape of the Bragg peaks and thus calculate the correlation length by 2/fwhm. As mentioned above, our calculation was done with the assumption of a liquidlike order, which is based on the line shape analysis. If we had used the Scherrer formula for our calculations, we would have arrived at crystallite sizes that are ~3 times larger than the correlation lengthes ζ that we report above. Despite this discrepancy in the models that were used, the comparison of our result with the work of Kuhl et al. clearly shows that the degree of lateral correlation is reduced upon transferring a DSPE monolayer from the air−water interface onto a silicon wafer. Kjaer et al.[46] made the same conclusion when comparing the lateral correlation lengthes of arachidic acid on water and after transfer onto a substrate, respectively.

Lipopolymer Monolayers (DSPE−PEO). Having revealed in detail how the film structure of DSPE monolayers depends on the humidity and on the lateral transfer pressure, we now discuss the characterization of DSPE−PEO monolayers. Lipopolymers with different PEO chain lengths were chosen, to elucidate how the polar polymer chains affect the swelling capacity of the monolayers as well as the lateral ordering of the alkyl chains.

DSPE−PEO(350). Figure 7a shows the XR data measured from a DSPE−PEO(350) LB film, which was transferred under a lateral pressure of 42 mN/m. Upon increasing the humidity, a shift of the minimums toward smaller scattering vectors could be observed, as in the case of DSPE. However, the shift here is clearly more pronounced, which indicates a higher increase in the monolayer thickness. The experimental data could be fitted with a four-box model (cf. Figure 7b), in which the PEO layer is located between the boxes representing the SiO_x and lipid headgroup layers, respectively, and where the alkyl chains are facing the air. The complete set of fit parameters is given in Table 2, and the fit curves were included as solid lines in Figure 7a. Clearly, distinct polar and nonpolar regions with a significant contrast in the electron density do exist in this monolayer. This is evidenced by the irregular spacings of the fringes in the XR data. The increase in the monolayer thickness at high humidity is obviously due to the incorporation of water into the polar regions of the monolayer, i.e., the PEO and lipid headgroup layers. The total thickness increase was found to be 8 Å. As the electron density of water (334 nm^{-3}) is lower than those of PEO (397 nm^{-3}) and of the lipid headgroup, the electron density in the polar regions must decrease upon the incorporation of water. The expected change of the electron density can be calculated from the fitted densities for the dry monolayer in combination with the fitted thickness change upon increasing the humidity. The model parameters, which were fitted for the monolayer under high humidity, are again in quantitative agreement with the results from such calculations.

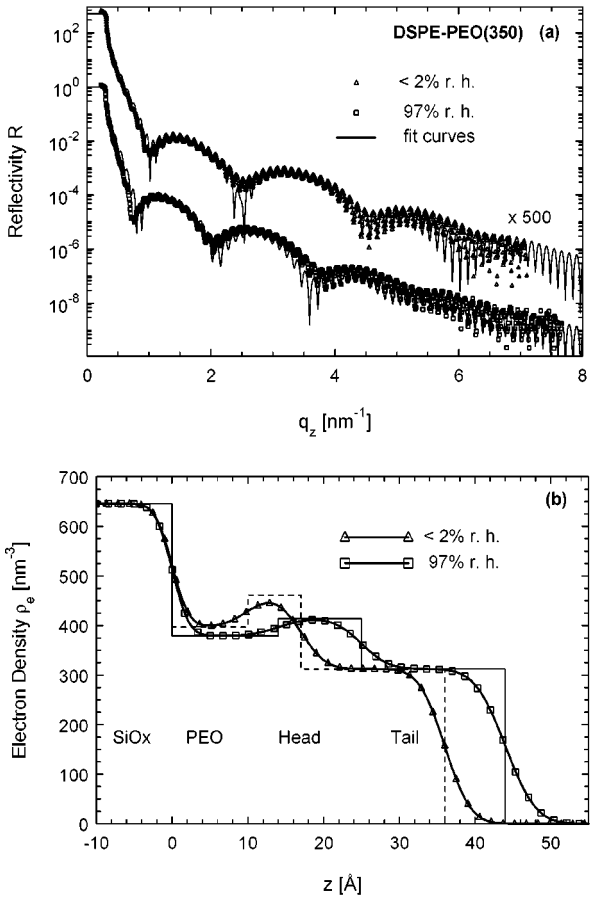

Figure 7. (a) XR data measured from an LB film of the lipopolymer DSPE−PEO(350) (π = 42 mN/m) under controlled humidity. (b) Shows the electron density profiles that correspond to the respective fit curves. The PEO layer is located between the substrate and the phosphate headgroup layer. The phosphate headgroup and the polymer layer are hydrated, and the film thickness increases by 8.0 Å. Concomitantly, the electron density in those regions decreases.

The length of the box that represents the alkyl chains was fitted to 19 Å, independent of humidity. This value is smaller than the length of a stretched C_{17} alkyl chain (21.7 Å; see above). So one might conclude that the lipid tails are slightly tilted away from the substrate surface normal. q_z-Resolved GIXD data reported by Kuhl et al.[27] gave clear evidence that the alkyl chains are tilted when DSPE−PEO(350) is floating on a water surface. On the other hand, the monolayer structure might change upon LB transfer on a silicon wafer, so one should be careful with a direct comparison of the results. Unfortunately, we have no such q_z-resolved diffraction data from the transferred films. We can assume a chain tilt only based on the XR data, i.e., due to the discrepancy between the fitted length of the alkyl chain box and the calculated length of the entirely stretched alkyl chain. Helm et al.[19] used the same reasoning when making conclusions about the alkyl chain tilt in a floating lipid monolayer. It is also noteworthy that the interface and surface roughness in the DSPE−PEO(350) film is only very slightly increased compared to DSPE. It may thus be concluded that the presence of this rather short polymer does not induce a significant disorder within the monolayer.

As in the case of DSPE, we have checked for the reversibility of water incorporation into the DSPE−PEO(350) monolayer.

(46) Kjaer, K.; Als-Nielsen, J.; Helm, C. A.; Tippmann-Krayer, P.; Möhwald, H. *Thin Solid Films* **1988**, *159*, 17−28.

Table 2. Fitted Structural Parameters of the DSPE−PEO Lipopolymer Monolayers as a Function of the PEO Chain Length and of the Adjusted Relative Humidity (r.h.)

	DSPE–PEO(350) $\pi = 42$ mN/m <2% r.h.	DSPE–PEO(350) $\pi = 42$ mN/m 97% r.h.	DSPE–PEO(750) $\pi = 42$ mN/m 97% r.h.	DSPE–PEO(2000) $\pi = 42$ mN/m 97% r.h.
		Electron Density ρ_e (nm^{-3})		
Si	703	703	703	703
SiO_x	646	646	646	667
PEO	397	379	355	360
head	461	414	426	390
tail	312	312	323	341
		Interface Roughness σ (Å)		
Si/SiO_x	1.5	1.5	1.5	1.5
SiO_x/PEO	2.5	2.5	2.3	3.0
PEO/head	3.6	4.0	3.0	7.0
head/tail	3.6	4.0	3.0	7.0
tail/air	3.8	4.5	3.5	5.2
		Layer Thickness d (Å)		
SiO_x	517.0	517.0	516.0	492.0
PEO	10.0	14.0	25.5	50.0
head	7.0	11.0	11.5	12.0
tail	19.0	19.0	17.5	18.0
total	36.0	44.0	54.5	80.0

Figure 5b compares the experimental data that were measured from the dry film with those obtained from the same film after it had been kept under 97% relative humidity for ∼20 h and subsequently reequilibriated in the initial dry environment. Apart from minor differences, both curves are essentially well reproduced. In particular, there is no significant difference in the overall decay of the curves. It is thus fair to conclude that the swelling of the lipopolymer monolayer is a reversible process, in which not only the original film thickness but also the low film roughness is being restored.

DSPE−PEO(750) and DSPE−PEO(2000). While the humidity-dependent XR curves from DSPE and DSPE−PEO(350) monolayers show qualitatively the same trends, the data obtained from DSPE−PEO(750) and from DSPE−PEO(2000) are markedly different. As shown in panels a and b of Figure 8, the periodicities of the Kiessig fringes in the respective XR curves do not significantly increase when the samples are exposed to high humidity. In particular, the angular positions of the first minimums are hardly changed. (Note that the shallow first minimum in case of the dry monolayers could only be observed after taking careful measures to minimize radiation damage as already pointed out above). This is surprising because, as already discussed for the DSPE and DSPE−PEO(350) monolayers, any thickness change shows up in a concomitant change of the periodicity in the XR curves. On the other hand, a pronounced increase in the depth of the minimums is clearly observed upon increasing the humidity, which indicates that the electron density contrast within the monolayers does change. So far we could not find a fit model that may quantitatively describe the experimental data both under dry conditions and at high humidity in a consistent way.

For the monolayers under high humidity, reasonable structural models could be established, which will be discussed in the following. In case of DSPE−PEO(750) transferred at 42 mN/m, clearly irregular spacings in the Kiessig fringes were observed (cf. Figure 9a). As pointed out above, this indicates a well-defined monolayer structure with a significant internal contrast. The data were fitted with a four-layer model (cf. inset in Figure 9a and Table 2), as in the case of DSPE−PEO(350).

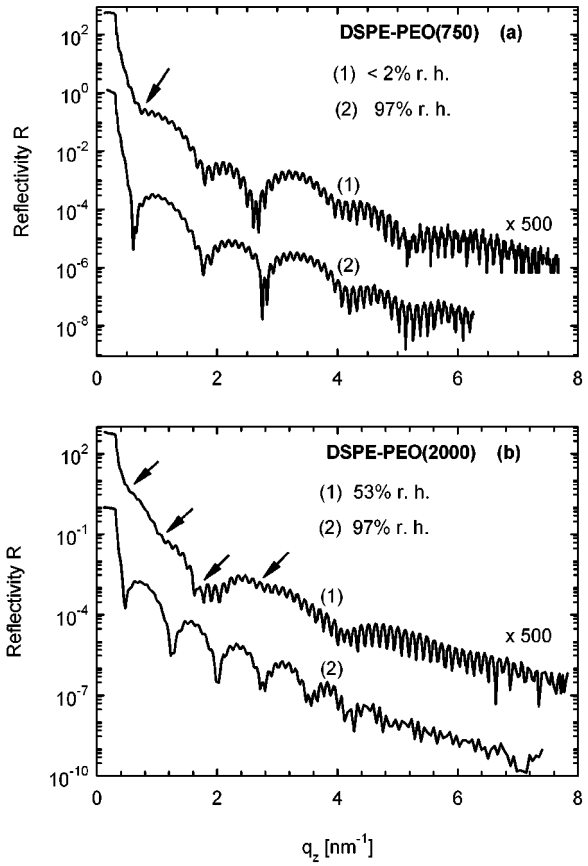

Figure 8. XR data measured from an LB film of (a) DSPE−PEO(750) ($\pi = 42$ mN/m) and (b) DSPE−PEO(2000) ($\pi = 42$ mN/m) under controlled humidity. Note the shallow minimums that were observed under dry conditions (indicated by arrows). Surprisingly, their angular positions indicate that the respective dry films have a thickness which is comparable to that of the same film under high humidity. Upon increasing the humidity, a significant change of electron density occurs within the film (as evidenced by the deeper minimums observed under high humidity), even though the film thickness remains nearly unchanged.

The total monolayer thickness was determined to 54.5 Å, which is 10.5 Å thicker than the DSPE−PEO(350) monolayer under the same condition. Due to the relatively high electron density

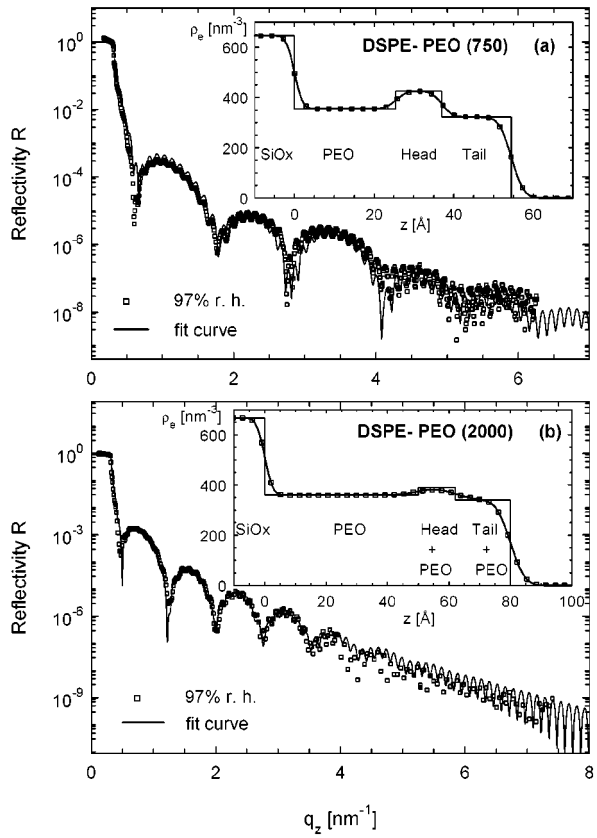

Figure 9. XR data measured from LB films of (a) DSPE−PEO(750) and (b) DSPE−PEO(2000) (π = 42 mN/m, respectively) at 97% relative humidity. The irregular spacings of the Kiessig fringes in (a) indicate that the DSPE−PEO(750) film exhibits a significant internal contrast. The phosphate headgroup and the polymer layer are located in distinct regions. The PEO layer resides between the substrate and the phosphate headgroup. On the other hand, the strictly regular spacings of the Kiessig fringes in (b) indicate that the DSPE−PEO(2000) film has a rather flat electron density profile without any pronounced internal contrast. The insets show the respective electron density profiles that correspond to the fit curves.

of the lipid headgroup, its position is clearly marked. The thickness of the hydrated polymer layer amounts to 25.5 Å, which is nearly half of the total layer thickness. The top layer, in which the alkyl chains are located, amounts to ∼17.5 Å, which is clearly smaller than the length of a stretched C_{17} chain. One may thus conclude that the chains are either tilted or not completely elongated. This may be explained by the bulkiness of the attached polymer chain, which creates a mismatch with respect to the size of the aliphatic tails. As a consequence of this mismatch, lateral PEO−PEO repulsions become significant. Such repulsions are also evident from the molecular area of DSPE−PEO(750) at the air−water interface, which was determined to 58 Å^2 under a lateral pressure of 42 mN/m. This value is significantly larger than that of DSPE (39 Å^2). On the other hand, for DSPE−PEO(350) at that high lateral pressure, the polymer chains may be compressed and elongated to such a degree that the molecular area (42 Å^2) is nearly equal to that of DSPE. Based on q_z-resolved, grazing incidence X-ray diffraction and XR data from a DSPE−PEO(750) monolayer at the air−water-interface, Kuhl et al.[27] came to the convincing conclusion that the tilt of the alkyl chains is very small under 42 mN/m. It was reported that the packing stress in the monolayer, which is induced by the bulky polymer chains, is relaxed through a staggering of the molecules in the vertical direction. As a consequence, significant intermixing of polymer with headgroup, headgroup with tail, and tail with air would occur. On the other hand, our XR data from the transferred monolayer are best fitted with rather low values for the various interface and surface roughness parameters σ (3−4 Å). In case of significant staggering, a considerably higher roughness would be expected at each interface. As we have no diffraction data from this sample so far, we cannot make unambiguous statements about the tilt and lateral ordering of the lipid tails.

The XR data measured under high humidity from the DSPE−PEO(2000) monolayer (transferred at 42 mN/m) exhibit several Kiessig fringes, with strictly regular spacings between all minimums (cf. Figure 9b). Obviously, the decaying XR curve is modulated by only a single frequency, beside that due to the SiO*x* layer. This is in contrast to all the other samples, where the Kiessig fringes are markedly irregular due to the superposition of several different modulation frequencies and amplitudes. From the existence of only one modulation frequency, one may conclude that the electron density gradients within the monolayer are rather small, so that the XR pattern is dominated by the superposition of X-rays that are reflected at the film surface and at the SiO_x−film interface, respectively. Thus, the total film thickness may directly be inferred from the observed oscillation frequency. It is determined to 80 Å, which is 25 Å thicker as compared to the DSPE−PEO(750) monolayer. And indeed, the best fit could be obtained with a rather flat electron density profile (cf. inset in Figure 9b and Table 2).

We have also investigated the DSPE−PEO(2000) monolayer by grazing incidence X-ray diffraction. Unfortunately, reliable data could be obtained only under high-humidity conditions. In the case of the dry monolayer, the shape and position of the observed Bragg peak could not sufficiently be reproduced in repeated scans. So those data had to be discarded. In the measurement under high humidity, we could find one diffraction peak (cf. Figure 6b), indicating a certain degree of alkyl chain ordering. From the width of the Lorentzian peak, the positional correlation length is calculated to 8 Å or two molecular diameters, only. It is surprising, however, that this peak was observed at the same angle position as that of the DSPE monolayer. The corresponding Bragg spacing amounts to 5.54 Å, and the area per lipopolymer molecule calculated from that value is 40 Å^2. This is much smaller than the molecular area of 91 Å^2 obtained from the pressure−area isotherm prior to the LB transfer. So obviously there exists a discrepancy that requires an explanation.

The same result was recently reported by Ahrens et al.,[25] where the diffraction peaks from DSPE and DSPE−PEO(2000) monolayers floating at the air−water interface were observed at nearly identical positions, despite the attached bulky polymer chain in the lipopolymer. They gave strong evidence that this may be explained by a laterally inhomogeneous monolayer structure, where hydrophobic nanodomains formed by closely packed alkyl chains are immersed into the hydrated polymer (cf. Figure 3 in ref 25). If those lateral inhomogeneities evolve on a length scale smaller than the coherence length of the radiation, a rather low variation of the electron density along the film surface normal would be expected, because X-ray reflectivity then probes laterally averaged electron density profiles. As explained above, we found that the variation of the electron density within the transferred DSPE−PEO(2000)

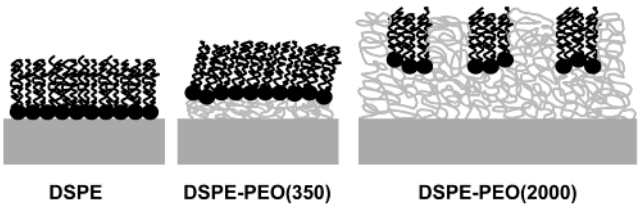

Figure 10. Schematic drawings of the suggested monolayer structures at 97% relative humidity.

film is very small indeed. In addition, the surface roughness (∼5 Å) and interface roughness (∼7 Å) that we have determined for this sample was highest among all investigated monolayers. All these findings suggest that the films at the air−water-interface and on the substrate could exhibit similar structures. Our XR data as well as the diffraction data can be explained by such a model. Figure 10 shows the proposed monolayer structure under high humidity in a very schematic way.

Until now, we could not find a structural model for the DSPE−PEO(750) and DSPE−PEO(2000) monolayers in a dry environment that can properly describe the XR data. As already discussed in connection with Figure 8, those monolayers have the peculiar feature that upon increasing the humidity the monolayer thickness seems to change only very little, whereas the internal contrast changes considerably. One could thus speculate that the polymer chains are very loosely packed in the dry polymer film, with a concomitant low electron density in the polymer region and a high thickness. Upon exposing this monolayer to high humidity, water could replace the air in the polymer layer, which leads to a significant change in the electron density, without affecting the monolayer thickness. Qualitatively, the experimental data could be understood in this way; however, the corresponding fit curves cannot fully describe all curve features, in particular the depth of the first minimum. Further characterization with complementary methods is needed to obtain more structural information.

Summary

An X-ray reflectivity and diffraction study on the structures of lipid and lipopolymer monolayers under controlled humidity was presented. With increasing PEO chain length, a systematic increase in the periodicities of the oscillations in the XR curves was observed, indicating an increasing film thickness (cf. Tables 1 and 2). Highly regular spacings in the Kiessig fringes were measured for DSPE−PEO(2000), as opposed to the irregular spacings observed for all other samples. From this it could be concluded that all films except the DSPE−PEO(2000) monolayer exhibit distinct layers in which the polymer cushion, the lipid headgroup, and the lipid tails are located. The presence of the hydrophilic polymer cushion between the solid substrate and the lipid moieties results in an increased swelling capacity under high humidity. It could be shown that the incorporation of water into the monolayers of DSPE and DSPE−PEO(350) is a reversible process. In the case of the DSPE monolayer, the degree of lateral order increases considerably upon increasing the humidity. Significant intermixing and the immersion of the lipid moieties into the polymer layer occurs in the DSPE−PEO-(2000) film.

Acknowledgment. Synchrotron radiation experiments at SPring-8 were performed in cooperation with the Japan Synchrotron Radiation Research Institute (JASRI, Proposal 2000B0041-ND -np). The allowed beam time there is gratefully acknowledged. J.B. also gratefully acknowledges beam time at the Pohang Light Source (PLS) in Korea, where part of the reflectivity data were collected under Proposal 2000-2036-017.

Supporting Information Available: Chemical structures of the lipid and lipopolymers that were used; pressure−area isotherms measured prior to LB transfer; detailed explanations of sample preparation and data collection procedures; a schematic of the sample cell that was designed for the measurements under controlled humidity; a representative comparison of the intensities measured in specular and off-specular scans; basic theory of XR and GIXD and fitting procedures; an example for how radiation damage affects the XR curves; a direct comparison of the XR data of all investigated monolayers at high and low humidity. This material is available free of charge via the Internet at http://pubs.acs.org. See any current masthead page for ordering information and Web access instructions.

JA0265308